

Article

Hydrochemistry of Medium-Size Pristine Rivers in Boreal and Subarctic Zone: Disentangling Effect of Landscape Parameters across a Permafrost, Climate, and Vegetation Gradient

Oleg S. Pokrovsky ^{1,*} , Artem G. Lim ² , Ivan V. Krickov ² , Mikhail A. Korets ³ , Liudmila S. Shirokova ^{1,4} and Sergey N. Vorobyev ²

¹ GET, UMR 5563, CNRS, University of Toulouse (France), 14 Avenue Edouard Belin, 31400 Toulouse, France; liudmila.shirokova@get.omp.eu

² BIO-GEO-CLIM Laboratory, Tomsk State University, Lenina Av., 36, 634050 Tomsk, Russia; lim_artiom@mail.ru (A.G.L.); krickov_ivan@mail.ru (I.V.K.); soil@green.tsu.ru (S.N.V.)

³ V.N. Sukachev Institute of Forest of the Siberian Branch of Russian Academy of Sciences, KSC SB RAS, 660036 Krasnoyarsk, Russia; mik@ksc.krasn.ru

⁴ N.P. Laverov Federal Center for Integrated Arctic Research, UrB Russian Academy of Science, 23 Nab Severnoi Dviny, 163000 Arkhangelsk, Russia

* Correspondence: oleg.pokrovsky@get.omp.eu



Citation: Pokrovsky, O.S.; Lim, A.G.; Krickov, I.V.; Korets, M.A.; Shirokova, L.S.; Vorobyev, S.N. Hydrochemistry of Medium-Size Pristine Rivers in Boreal and Subarctic Zone: Disentangling Effect of Landscape Parameters across a Permafrost, Climate, and Vegetation Gradient. *Water* **2022**, *14*, 2250. <https://doi.org/10.3390/w14142250>

Academic Editor: Maurizio Barbieri

Received: 29 June 2022

Accepted: 14 July 2022

Published: 18 July 2022

Publisher's Note: MDPI stays neutral with regard to jurisdictional claims in published maps and institutional affiliations.



Copyright: © 2022 by the authors. Licensee MDPI, Basel, Switzerland. This article is an open access article distributed under the terms and conditions of the Creative Commons Attribution (CC BY) license (<https://creativecommons.org/licenses/by/4.0/>).

Abstract: We studied two medium size pristine rivers (Taz and Ket) of boreal and subarctic zone, western Siberia, for a better understanding of the environmental factors controlling major and trace element transport in riverine systems. Our main objective was to test the impact of climate and land cover parameters (permafrost, vegetation, water coverage, soil organic carbon, and lithology) on carbon, major and trace element concentration in the main stem and tributaries of each river separately and when considering them together, across contrasting climate/permafrost zones. In the permafrost-bearing Taz River (main stem and 17 tributaries), sizable control of vegetation on element concentration was revealed. In particular, light coniferous and broadleaf mixed forest controlled DOC, and some nutrients (NO₂, NO₃, Mn, Fe, Mo, Cd, Ba), deciduous needle-leaf forest positively correlated with macronutrients (PO₄, P_{tot}, Si, Mg, P, Ca) and Sr, and dark needle-leaf forest impacted N_{tot}, Al, and Rb. Organic C stock in the upper 30–100 cm soil positively correlated with Be, Mn, Co, Mo, Cd, Sb, and Bi. In the Ket River basin (large right tributary of the Ob River) and its 26 tributaries, we revealed a correlation between the phytomass stock at the watershed and alkaline-earth metals and U concentration in the river water. This control was weakly pronounced during high-water period (spring flood) and mostly occurred during summer low water period. Pairwise correlations between elements in both river systems demonstrated two group of solutes—(1) positively correlated with DIC (Si, alkalis (Li, Na), alkaline-earth metals (Mg, Ca, Sr, Ba), and U), this link originated from groundwater feeding of the river when the labile elements were leached from soluble minerals such as carbonates; and (2) elements positively correlated with DOC (trivalent, tetravalent, and other hydrolysates, Se and Cs). This group reflected mobilization from upper silicate mineral soil profile and plant litter, which was strongly facilitated by element colloidal status, notably for low-mobile geochemical tracers. The observed DOC vs DIC control on riverine transport of low-soluble and highly mobile elements, respectively, is also consistent with former observations in both river and lake waters of the WSL as well as in soil waters and permafrost ice. A principal component analysis demonstrated three main factors potentially controlling the major and TE concentrations. The first factor, responsible for 26% of overall variation, included aluminum and other low mobile trivalent and tetravalent hydrolysates, Be, Cr, Nb, and elements strongly complexed with DOM such as Cu and Se. This factor presumably reflected the presence of organo-mineral colloids, and it was positively affected by the proportion of forest and organic C in soils of the watershed. The second factor (14% variation) likely represented a combined effect of productive litter in larch forest growing on carbonate-rich rocks and groundwater feeding of the rivers and acted on labile Na, Mg, Si, Ca, P, and Fe(II), but also DOC, micronutrients (Zn, Rb, Ba), and phytomass at the watershed. Via applying a substituting space for time approach for south-north gradient of studied river basins, we predict that

climate warming in northern rivers may double or triple the concentration of DIC, Ca, Sr, U, but also increase the concentration of DOC, POC, and nutrients.

Keywords: metals; carbon; nutrients; trace elements; landscape; permafrost; river; watershed; boreal

1. Introduction

Climate change, which is mostly pronounced in high latitudes, strongly impacts the chemistry of rivers and streams and can bring yet unknown consequences on carbon, nutrient, and metal export from land to ocean thus enhancing the retroactive link to climate change drivers [1–4]. There are numerous case studies of climate change impact on surface and groundwater sustainability and hydrochemistry, such as those performed in temperate/subtropical regions [5,6]. However, huge northern unpopulated territories of the world remain poorly covered by a coupled hydrochemical/hydrological approach. This is especially true for pristine permafrost-bearing regions located at high latitudes and containing sizable amount of carbon in the form of peat, organic litter, and vegetation. An example is Western Siberian Lowland (WSL), located in the gradient of climate and permafrost zones within essentially the same lithological background, minimal variations in river runoff and relief and moderate to negligible anthropogenic activity. The interest of the WSL is that it contains huge peat resources and presents rather shallow, essentially discontinuous to sporadic/isolated permafrost, highly vulnerable to thawing [7–10]. For this relatively large territory (2 million km²), extensive studies of small [11–19] and large [20] river dissolved, colloidal and particulate load, chemical composition of soil ice and suprapermafrost waters [21–24], and gaseous regime of rivers and lakes [25–27] have been performed. However, the majority of these studies except that of the Ob River [20] dealt with single site sampling of a given river, without addressing the spatial variability of riverine solutes within a watershed. This is a clear shortcomings of current state of knowledge of western Siberian rivers, because without sufficient spatial coverage, one cannot test the impact of various landscape factors on water hydrochemistry within the same river basin.

In the present study, we used a coupled hydrochemical/landscape (land cover) approach that allows revealing the main environmental factors controlling the hydrochemical composition of the river water. Up to now, such an approach has been efficiently used only for single-point sampling of small rivers [13–19] and one large Siberian River [20] but has not been implemented at the scale of the whole watershed of medium-size rivers. Toward better understanding of land cover control on riverine C, nutrient and metal transport, we chose two medium size rivers of western Siberia, Taz ($S_{\text{watershed}} = 150,000 \text{ km}^2$) and Ket ($S_{\text{watershed}} = 95,000 \text{ km}^2$) located within permafrost-bearing forest-tundra/tundra and permafrost-free taiga biomes, respectively. Both rivers drain through similar sedimentary deposits overlaid by peatland and forest/tundra; they are virtually pristine (population density $< 1 \text{ people km}^{-2}$) and have no industrial or agricultural activity on their watershed. Within the on-going drastic climate change in Siberia, the southern river (Ket) can be considered as an extreme scenario of long-term transformation of the northern River (Taz) in case of complete disappearance of discontinuous permafrost and northward migration of the taiga forest. Therefore, our primary objective in this work was to test the impact of climate and land cover parameters (permafrost, vegetation, water coverage, soil organic carbon, and lithology), on carbon, major and trace element concentration in the main stem and tributaries of each river separately and when considering them together, across contrasting climate/permafrost zones. A flowchart of methodology and approach used in the present study is illustrated in Figure 1. We anticipate that, via employing similar approach for two sufficiently contrasting and yet representative river basin of the WSL, we can provide essential information for coupled land—River C, nutrient and metal fluxes for climate modeling of the region and to foresee future, long-term changes in much large territory

of strongly understudied permafrost-affected Eurasian lowlands, which includes North Siberia, Anabar, Kolyma and Yana-Indigirka lowlands, with an overall territory more than 2 million km².

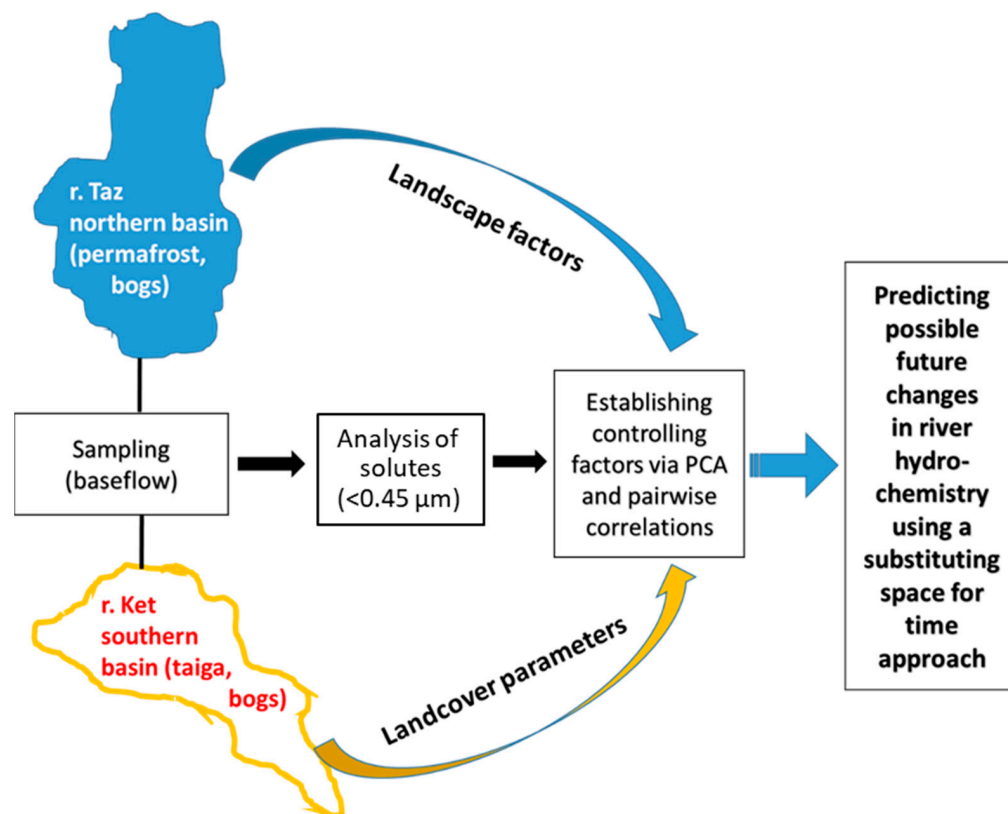


Figure 1. A flow chart of methodological approach used in the present study.

2. Study Site and Methods

2.1. Ket River Basin

We sampled the Ket River main stem and its 26 tributaries during the peak of the spring flood and the end of summer baseflow. The catchment area of sampled watersheds ranged from 94,000 km² (Ket's mouth) to 20 km² (smallest tributary). The studied watersheds presented rather similar lithology, climate, and vegetation, given its generally west—east orientation, Figure 2; Ref. [28]). The Ket River basin (right tributary of the Ob River) is poorly accessible and can be considered as essentially pristine comprising about 50% forest and 40% of wetlands while having virtually negligible agricultural and forestry activity. The river basin is poorly populated (0.27 person km⁻²) and, compared to left tributaries of the Ob River, lacks road infrastructure due to absence of hydrocarbon exploration activity. We therefore consider this river as a model one for medium size rivers of the boreal zone of western Siberia Lowland covered by forests and bogs. As such, the results on river water hydrochemistry obtained from this watershed can be extrapolated to much larger territory, comprising several million km² of permafrost-free taiga forest and bog biome, extending over 3000 km between the left tributaries of the Yenisei River in the east and Finland in the west. The mean annual air temperatures (MAAT) of the Ket River basin is -0.75 ± 0.15 °C and the mean annual precipitation is 520 ± 20 mm y⁻¹. The lithology is represented by silts and sands with carbonate concretions overlaid by quaternary deposits (loesses, fluvial, glacial, and lacustrine deposits). The dominant soils are podzols in forest areas and histosols in peat bog regions.

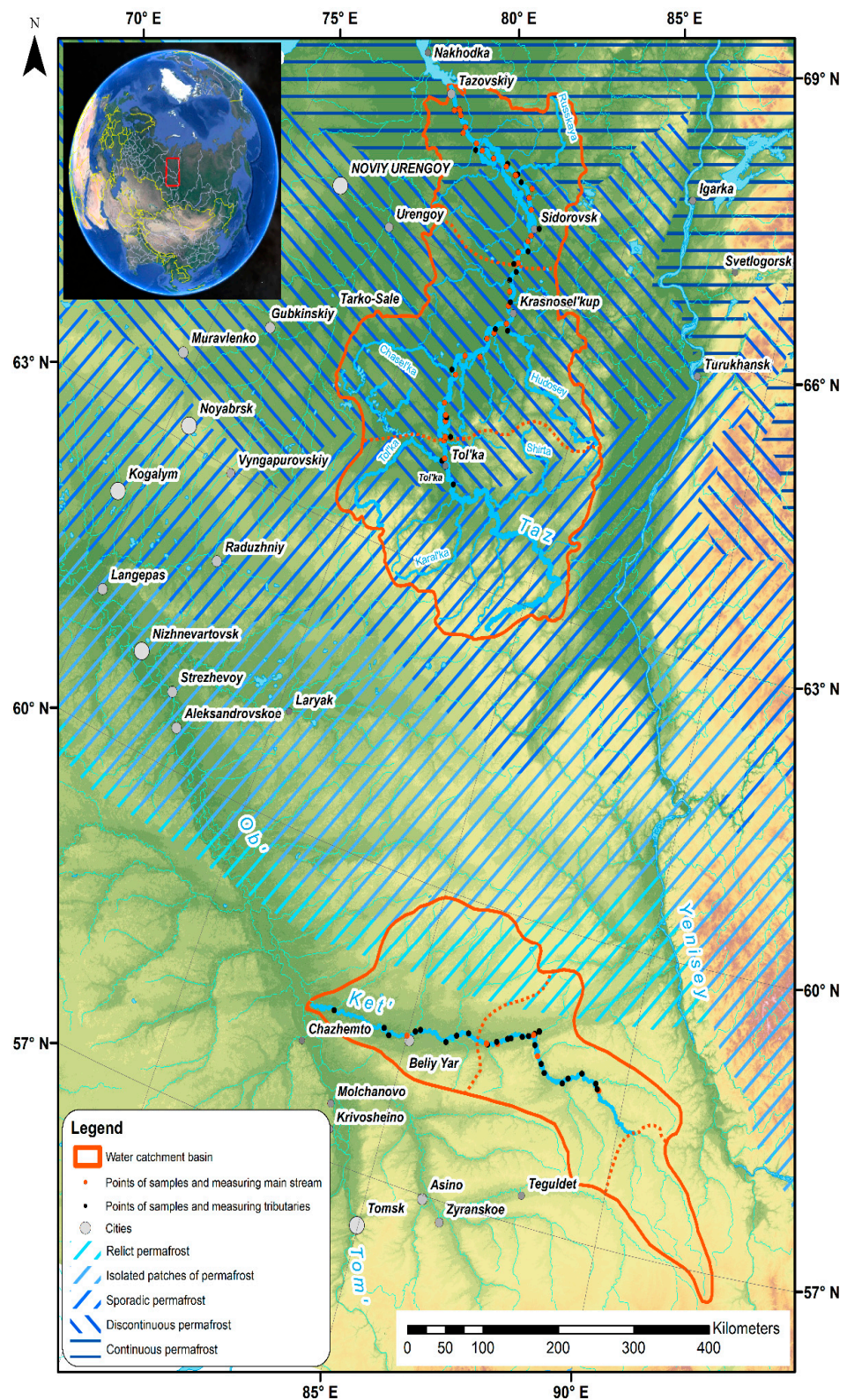


Figure 2. Map of the two studied river basins (Taz in the north and Ket in the south). The sampling points of the main stem and tributaries are shown by red and black circles, respectively.

2.2. Taz River Basin

The Taz River sampled in this work included the main stem and its 17 tributaries whose catchment area ranged from 149,000 km² at the Taz's mouth to 25 km² of smallest

sampled tributary. Alike the Ket River basin, all sampled catchments exhibited similar lithology (clays, silts and sands overlaid by quaternary loesses, fluvial, glacial, and lacustrine deposits), but more contrasting climate and vegetation due to its north to south orientation (Figure 2). The MAAT ranges from -4.6 °C in the headwaters (Tolka village) to -5.4 °C in the low reaches (Tazovskiy town). The mean annual precipitation is 500 mm y^{-1} in the central part of the basin (Krasnoselkup) and 600 mm y^{-1} in the low reaches of the Taz River. Given its landscape and climate features, the Taz River basin includes: (1) the upper (southern) part (“headwaters”) which comprises 400–800 km upstream of the river mouth, where the permafrost is sporadic to discontinuous and the dominant vegetation is forest-tundra and taiga, and (2) the low reaches (northern) part, located 0–400 km upstream of the mouth where the permafrost is continuous to discontinuous and the dominant biome is tundra and forest-tundra.

2.3. Sampling

For the Ket River, the peak of annual discharge in 2019 occurred in the end of May whereas in August, the discharge was three to five times lower. From 18 May to 28 May 2019, and from 30 August to 2 September 2019, we started the boat trip in the middle course of the Ket River (Beliy Yar), and moved, first, 475 km upstream the Ket River till its most headwaters, and then moved 834 km downstream till the river mouth. We stopped each 50 km along the Ket River and sampled for major hydrochemical parameters, suspended matter, and bacteria. We also moved several km upstream of selected tributaries to sample for river hydrochemistry.

In the Taz River, the peak of annual discharge in 2019 occurred in the middle of June (5600 m³ s⁻¹; in August, the discharge was 5 times lower). Therefore, the month of July (average discharge is 2300 m³ s⁻¹; range 1920 – 3370 m³ s⁻¹) can be considered as the end of spring flood period. From 12 July to 16 July 2019 we moved 800 km downstream the Taz River from its most headwaters (Tolka village) to the low reaches (Tazovskiy town). We stopped each ~50 to 100 km of the boat route and sampled for hydrochemical parameters, river suspended matter and total bacterial number of the main stem. For sampling the tributaries, we moved 500–1500 m upstream of the confluence zone.

2.4. Analyses

The dissolved oxygen (CellOx 325; accuracy of $\pm 5\%$), specific conductivity (TetraCon 325; $\pm 1.5\%$), and water temperature (± 0.2 °C) were measured in situ at 20 cm depth using a WTW 3320 Multimeter. The pH was measured using portable Hanna instrument via combined Schott glass electrode calibrated with NIST buffer solutions (4.01, 6.86, and 9.18 at 25 °C), with an uncertainty of 0.01 pH units. The river water was sampled in pre-cleaned polypropylene bottle from 20–30 cm depth in the middle of the river and immediately filtered through disposable single-use sterile Sartorius filter units (0.45 μ m pore size). The first 20 mL of filtrate was discarded. The DOC and dissolved inorganic carbon (DIC) were determined by a Shimadzu TOC-VSCN Analyzer (Kyoto, Japan) with an uncertainty of 3% and a detection limit of 0.1 mg/L. Blanks of Milli-Q water passed through the filters demonstrated negligible release of DOC from the filter material. Specific ultraviolet absorbance (SUVA₂₅₄) was measured via ultraviolet absorbance at 254 nm using a 10-mm quartz cuvette on a Bruker CARY-50 UV-VIS spectrophotometer and divided by the concentration of DOC (L mg⁻¹ m⁻¹). The concentrations of C and N in suspended material (particulate organic carbon and nitrogen (POC and PON, respectively)) were determined via filtration of 1 to 2 L of freshly collected river water (at the river bank or in the boat) with pre-weighted GFF filters (47 mm, 0.8 μ m) and Nalgene 250-mL polystyrene filtration units using a Mityvac[®] manual vacuum pump. Particulate C and N were measured using catalytic combustion with Cu-O at 900 °C with an uncertainty of $\leq 0.5\%$ using Thermo Flash 2000 CN Analyzer at EcoLab, Toulouse. The samples were analyzed before and after 1:1 HCl treatment to distinguish between total and inorganic C; however, the ratio of C_{organic}:C_{carbonate} in the river suspended matter (RSM) was always above 20 and the

contribution of carbonate C to total C in the RSM was equal in average $0.3 \pm 0.3\%$ (2 s.d., $n = 30$).

Total microbial cell concentration was measured after sample fixation in glutaraldehyde, by flow cytometry (Guava[®] EasyCyte™ systems, Merck, Darmstadt, Germany). Cells were stained using 1 μL of a 10 times diluted SYBR GREEN solution (10000 \times , Merck), added to 250 μL of each sample before analysis. Particles were identified as cells based on green fluorescence and forward scatter [29].

All analytical approaches used in this study for major and trace element analyses followed methods developed for western Siberian organic-rich surface waters [17,30,31]. The samples were preserved via refrigeration 1 month prior to analysis. Major anion (Cl , SO_4^{2-}) concentrations were measured by ion chromatography (HPLC, Dionex ICS 2000) with an uncertainty of 2%. International certified samples ION, PERADE, and RAIN were used for validation of the analyses. Major cations (Ca, Mg, Na, K), Si, and ~40 trace elements were determined with an Agilent iCap Triple Quad (TQ) ICP MS using both argon and helium modes to diminish interferences. About 3 $\mu\text{g L}^{-1}$ of In and Re were added as internal standards along with three various external standards. Detection limits of TE were determined as $3\times$ the blank concentration. The typical uncertainty for elemental concentration measurements ranged from 5–10% at 1–1000 $\mu\text{g/L}$ to 10–20% at 0.001–0.1 $\mu\text{g/L}$. The Milli-Q field blanks were collected and processed to monitor for any potential contamination introduced by our sampling and handling procedures. The SLRS-6 (Riverine Water Reference Material for Trace Metals certified by the National Research Council of Canada) was used to check the accuracy and reproducibility of analyses [32,33]. Only those elements that exhibited good agreement between replicated measurements of SLRS-6 and the certified values (relative difference < 15%) are reported in this study.

2.5. Landscape Parameters and Water Surface Area of the Ket and Taz River Basin

The physio-geographical characteristics of the Ket and Taz tributaries and several sampling points of the main stem of both rivers were determined by applying available digital elevation model (DEM GMTED2010), soil, vegetation, and lithological maps. The landscape parameters were typified using TerraNorte Database of Land Cover of Russia (Ref. [34]; <http://terranorte.iki.rssi.ru>, accessed on 1 February 2020). This included various types of forest (evergreen, deciduous, needleleaf/broadleaf), grassland, tundra, wetlands, water bodies, and riparian zones. The climate parameters of the watershed were obtained from CRU grids data (1950–2016) [35] and NCSCD data (Ref [36]; doi:10.5879/ecds/00000001), respectively, whereas the biomass and soil OC content were obtained from BIOMASAR2 [37] and NCSCD databases. The lithology layer was taken from GIS version of Geological map of the Russian Federation (scale 1: 5,000,000, <http://www.geolkarta.ru/>, accessed on 1 February 2020).

2.6. Data Analysis

Element concentrations for all datasets were tested for normality using the Shapiro–Wilk test. In case of the data were not normally distributed, we used non-parametric statistics. Comparisons of major and trace element concentration in the main stem and the tributaries during two sampling seasons (Ket) and summer baseflow (Taz) were conducted using a non-parametric Mann Whitney test at a significance level of 0.05. For comparison of unpaired data, a non-parametric H-criterion Kruskal–Wallis test was used to reveal the differences between different seasons and between the main stem and tributaries. The Pearson rank order correlation coefficient ($p < 0.05$) was used to determine the relationship between major and trace element concentrations and main landscape parameters of several points of the main stem and all tributaries, as well as other potential drivers of TE concentrations in the river water such as pH, O_2 , water temperature, specific conductivity, DOC, SUVA (aromaticity), DIC, Fe, Al, particulate carbon and nitrogen, and total bacterial number.

3. Results and Discussion

3.1. Spatial and Seasonal Variation of Elements in the Ket River and Control of River Hydrochemistry by Landscape Parameters

All the primary data on dissolved ($<0.45 \mu\text{m}$) element concentration in both rivers together with relevant landscape parameters of the sampling points are available from the Mendeley Repository [28]. The spatial variations of element concentration in the main stem and tributaries of the Ket River were generally lower than the differences between the two seasons. This is illustrated by a plot of several major and trace elements along the full length of the river basin (Figure 3A–E), and further confirmed by a Mann–Whitney U test (Table S1 of the Supplementary Materials) which shows that the maximal differences in element concentrations are observed between seasons in both the main stem and the tributaries. The differences between the Ket River main stem and the tributaries were always lower or not pronounced for the same season. This allowed to calculate the mean concentrations of elements across the full length of the main stem and among all tributaries for each seasons (Figure S1 and Table S2 of the Supplementary Materials). Analyses of the differences in element concentration between the flood and the baseflow of the Ket River allowed distinguishing three group of solutes as illustrated in Figure 4. The first groups comprised elements having a factor of 2 to 10 higher concentrations in both main stem of the Ket River and tributaries during spring flood compared to summer baseflow, and included DOC, low soluble low mobile “lithogenic” hydrolysates (Be, Al, Ti, Cr, Ga, Y, Zr, Nb, REE, Hf, Bi, Th), some divalent heavy metals (Ni, Cu, Cd), oxyanions (Sb), Cs, Tl, and SO_4 . The second group typified highly mobile elements exhibiting lower concentrations during spring flood compared to the baseflow and included DIC, POC, alkaline and alkaline earth metals (Li, Na, Mg, Ca, Sr, Ba), labile nutrients (Si, P, Mn), oxyanions (As, Mo), Fe and U(VI). Finally, a group of elements demonstrated rather similar (within 30%) concentrations during both seasons and included Cl, micronutrients (V, Co, Zn, Se, Rb), Ge, W, and Cd.

A pairwise (Pearson) correlation of major and trace element concentration in the main stem and tributaries of the Ket River with main land cover parameters of the watershed was tested for both seasons, but notable correlations were observed only for the summer baseflow (Table S3). These correlations were detected only for alkaline-earth elements (Mg, Ca, Sr) and U, whose concentrations positively correlated ($R_{\text{Pearson}} \geq 0.5$; $p < 0.05$) with phytomass stock on the watersheds (Figure 5). However, the observed correlations do not necessarily indicate a direct control but may be the consequence of the fact that carbonate-bearing loesses are most favorable substrates for productive forests compared to clay, sand and peat-rich soils [20]. The carbonate minerals of these substrates are known to act as sizable sources of alkaline-earth metals and uranium [the latter is carried in the form of highly labile uranyl-carbonate complexes] in shallow subsurface and groundwater feeding the river during summer baseflow [16,17]. Other elements did not demonstrate any sizable correlations to the landscape factors. The most likely reason for paucity of such a control is highly homogeneous coverage of the river basins by forest, bogs, and riparian zones with essentially the same climate, runoff, vegetation, soil, and total phytomass stock, represented by similar tree species of the boreal taiga of permafrost-free zone of the WSL.

Overall, the dominance of the season over space in solute control in the river basin let us to consider, for further analysis, only the same season (summer baseflow) for both rivers. This allowed better understanding the main driving factors (landscape parameters) of dissolved major and trace element variation along the full length of the main stem of both rivers as well as within each river tributaries.

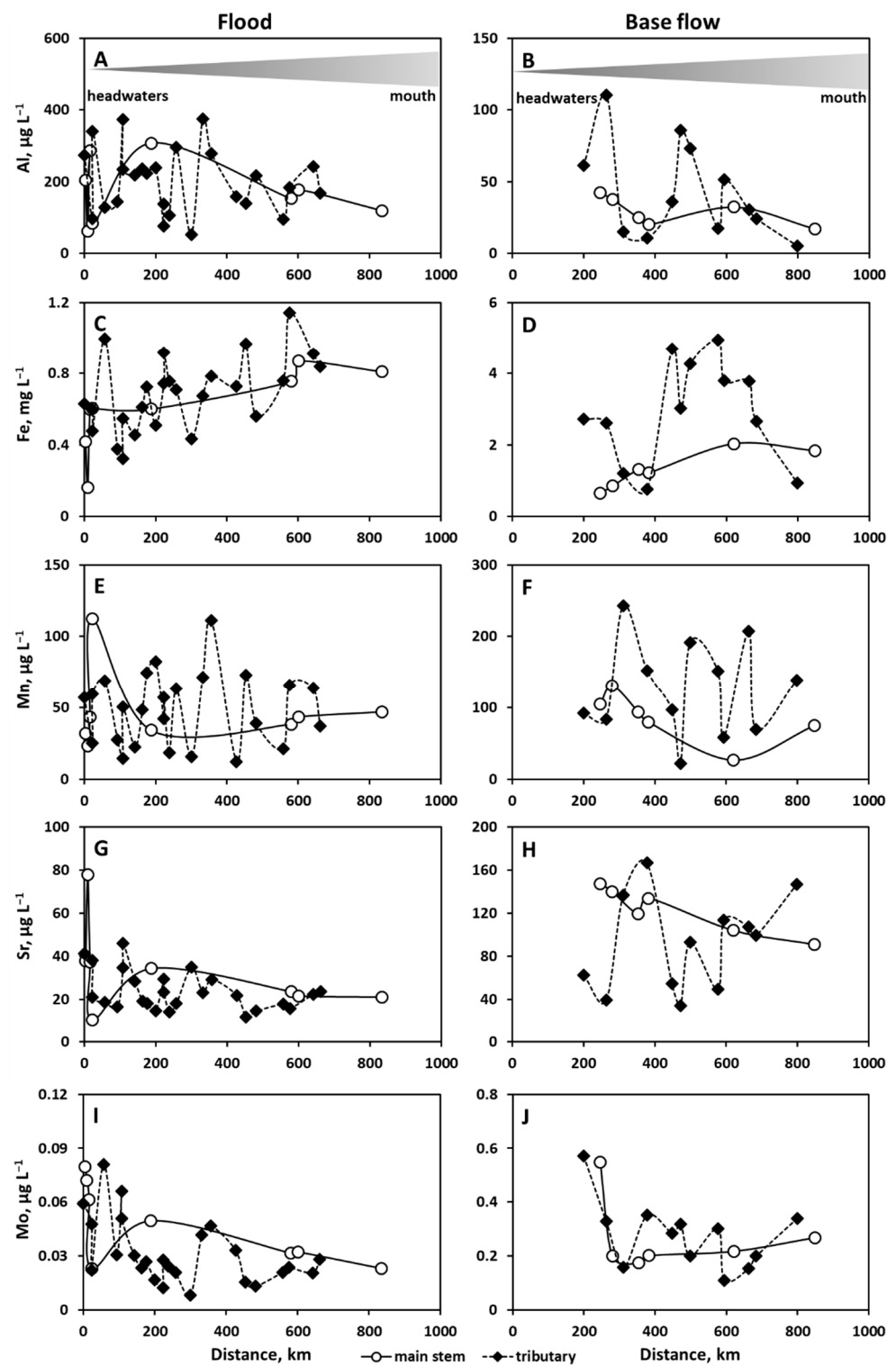


Figure 3. Al (A,B), Fe (C,D), Mn (E,F), Sr (G,H) and Mo (I,G) concentration in the Ket River main stem (open circles) and tributaries (solid diamonds) during spring flood (A,C,E,G,I) and summer baseflow (B,D,F,H,J).

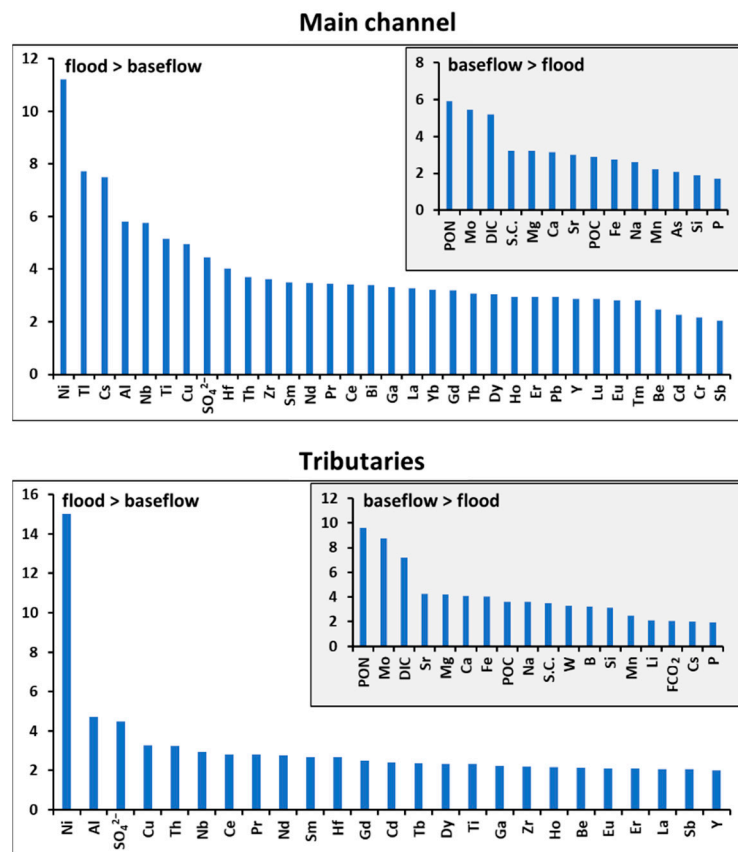


Figure 4. Mean ratio of element concentrations between spring flood period and summer baseflow in the Ket River main stem and tributaries.

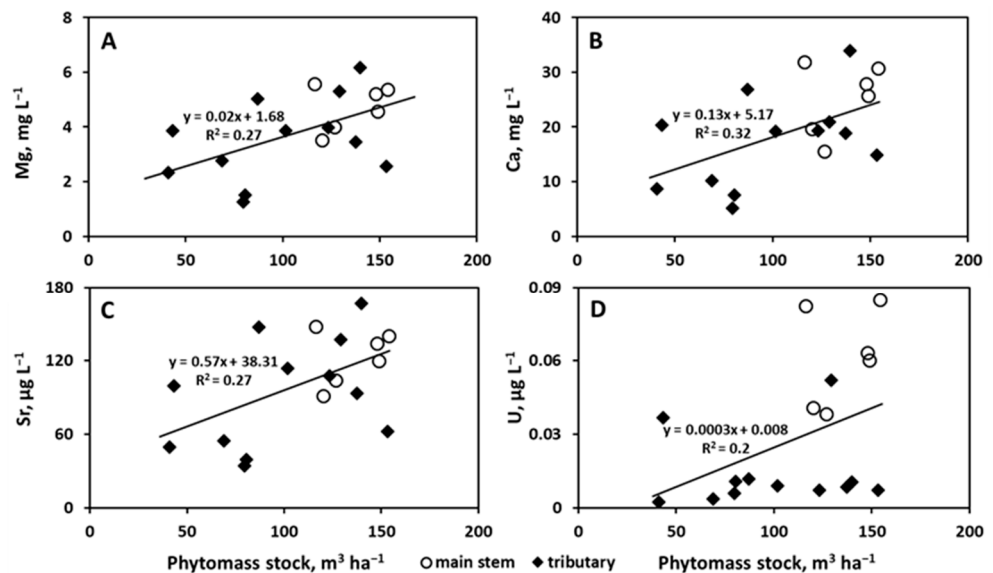


Figure 5. Example of positive correlations between Mg (A), Ca (B), Sr (C), and U (D) and landscape factors of the Ket River in summer.

3.2. Major and Trace Element Spatial Variation over the River Main Stem and among Tributaries of the Taz River Basin and Land Cover Control

The variations of major and trace element concentration along the Taz River were also rather low as illustrated in a plot of some major and trace element concentrations over the river distance, from the headwaters to the mouth (Figure 6). The concentration of DOC,

P_{tot} , NO_3 , NO_2 , Al, Fe, Cd, Ba, and Bi increased southward, with an increase in mean annual temperature. In contrast, in the northward direction, with an increase in tundra and discontinuous permafrost coverage, the concentrations of Cl, SO_4 , Li, B, Na, K, V, Ni, Cu, Y, REE, and U increased, which may stem from a combination of sea-salts release from the underlying marine clays and silts and far-range (>300 km) atmospheric transfer from the Norilsk smelters (V, Ni, Cu). The variations among tributaries were generally larger but did not exhibit any systematic evolution between the upper and lower reaches of the Taz River basin (Table S4). Therefore, we can hypothesize that the primary factor controlling solute concentration in the tributaries is land cover (see Section 3.3 below). In the main stem and tributaries, the difference in dissolved element concentration between the upper (southern) and lower (northern) part of the river has not exceeded 20–30% which was often within the standard deviation of the mean values. The only exception is Mn concentrations in the tributaries were two times higher in the south compared to the north.

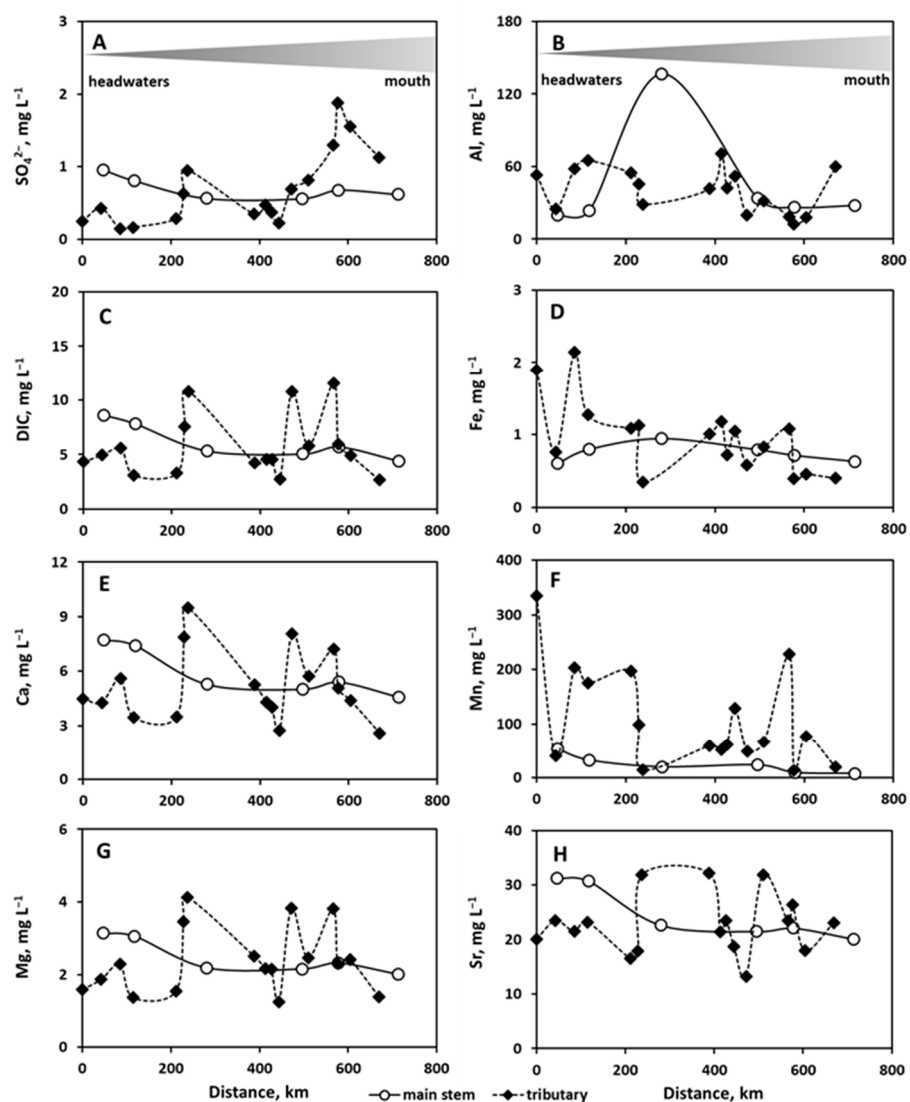


Figure 6. SO_4^{2-} (A), Al (B), DIC (C), Fe (D), Ca (E) Mn (F), Mg (G), and Sr (H) concentration in the Taz River main stem and tributaries during summer baseflow.

Pairwise correlations of major and trace element concentration in the Taz River basin with main physico-geographical, geocryological, and climatic features of the watershed revealed several potential drivers (Table S5). The tundra coverage of the watershed, corresponding to northward directions and proximity to the sea exhibited strong positive

($R_{\text{Pearson}} > 0.60$, $p < 0.01$) correlations with Li, B, Na, K, Cl, SO_4 , and U. These elements likely originate from sea salts of the former marine clays dominating the bedrocks of river catchments in the northern part of WSL [17] but also the deposition of marine aerosols in the form of snow [38]. The latter is also known to be enriched in Ni and Cu, reflecting the proximity of the low Taz reaches to the Norilsk Cu-Ni smelters in the northern part of WSL. This can explain positive ($R_{\text{Pearson}} > 0.50$, $p < 0.05$) correlations between the tundra coverage and the concentrations of Ni and Cu in the rivers of the Taz basin. Presumably, the atmospheric deposition of metal-rich aerosols can be transferred, via plant litter decay and surface runoff, to the river main stem and tributaries in the northern part of the basin.

The vegetation also exhibited notable impact on elements concentrations in the river water. Thus, presence of larch trees (deciduous needle-leaf forest coverage) positively correlated with concentrations of DOC and macronutrients (Si, Mg, Ca, Sr) and Cs. Light coniferous and broadleaf mixed forest positively impacted concentrations of DOC, macro- (PO_4 , NO_3 , NH_4) and micro-nutrients (Mn, Fe, Co, Mo, Ba, Cd). Finally, the organic carbon content in upper 0–30 and 0–100 cm of soil positively correlated with some micro-nutrients (Mn, Co, Mo) but also Be, Sc, Cd, Sb, and Bi. Noteworthy is that neither the watershed surface area nor the permafrost coverage, which are the two potential drivers of element geochemistry in surface waters i.e., [39–42], correlated with major and trace elements of the Taz River basin. Furthermore, we were not able to detect any control of other landscape features such as riparian zone, wetlands, and recent burns.

3.3. Common Features of Spatial Distribution of Major and Trace Element in Two River Basins during Summer

Analysis of pairwise correlations described in Sections 3.1 and 3.2 for two river basins individually revealed a number of common features in terms of apparent control of landscape parameters on element concentration in river waters. This allowed correlating the hydrochemical composition of the water column with major environmental factors that are likely to operate on both river basins as illustrated for some elements in Figure 7. The first factor is forest biomass in general and, in particular, the coverage of the watershed by larch trees (deciduous light needle leaf forest), which are most efficient for recycling the nutrients such as Li, B, Si, Zn, Rb, and Ba [43]. The second environmental parameter is bog coverage of the watershed, which was positively correlated with SUVA and low mobile lithogenic elements and divalent transition metals whose transport is facilitated by high DOC concentration (V, Ni, Cu, Y, heavy REE). The impact of bogs on retention of these elements was demonstrated in North European boreal rivers [44,45]. Noteworthy that the bog presence facilitated only the transport of heavy REE and not the light ones. In the WSL surface waters, the former are known to form much stronger complexes with allochthonous DOM from bogs and peat waters and less prone to be carried as organo-ferric colloids [30,46–48].

A small number of elements were associated with total bacterial number (SUVA, P, V, Fe, and As) and presumably marked shallow subsurface discharge of Fe(II)-rich waters from the adjacent peatlands and biotically driven formation of large size Fe hydroxide colloids, stabilized by allochthonous (aromatic) organic carbon. Strong co-precipitation of P, V, and As with Fe hydroxides is known from laboratory experiments with organic-rich (peatland) waters in the presence of soil and aquatic bacteria [49–52]. The area of riparian zones of the river positively correlated with DIC, Sr, Ba, U, and particulate organic nitrogen. While the first four elements could mark an enhanced discharge of deep and subsurface groundwaters in the riparian zones, notably of larger rivers, the correlation with PON could illustrate the generation of N-rich particles in the sediments of highly productive floodplains [13,18]. Among common climate parameters of both river basins, the precipitation did not impact the hydrochemical composition. However, the mean annual air temperature encompassed the contrast between northern and southern rivers and correlated with labile components of the river water (S.C., DIC, Li, B, Si, Ca, Sc, Zn, Se,

Rb, Sb, Cs, Ba, and U). This was fully consistent with previous observations of large (Ob, Ref. [20]; Lena, Ref. [53]) and small [15–17] Siberian rivers.

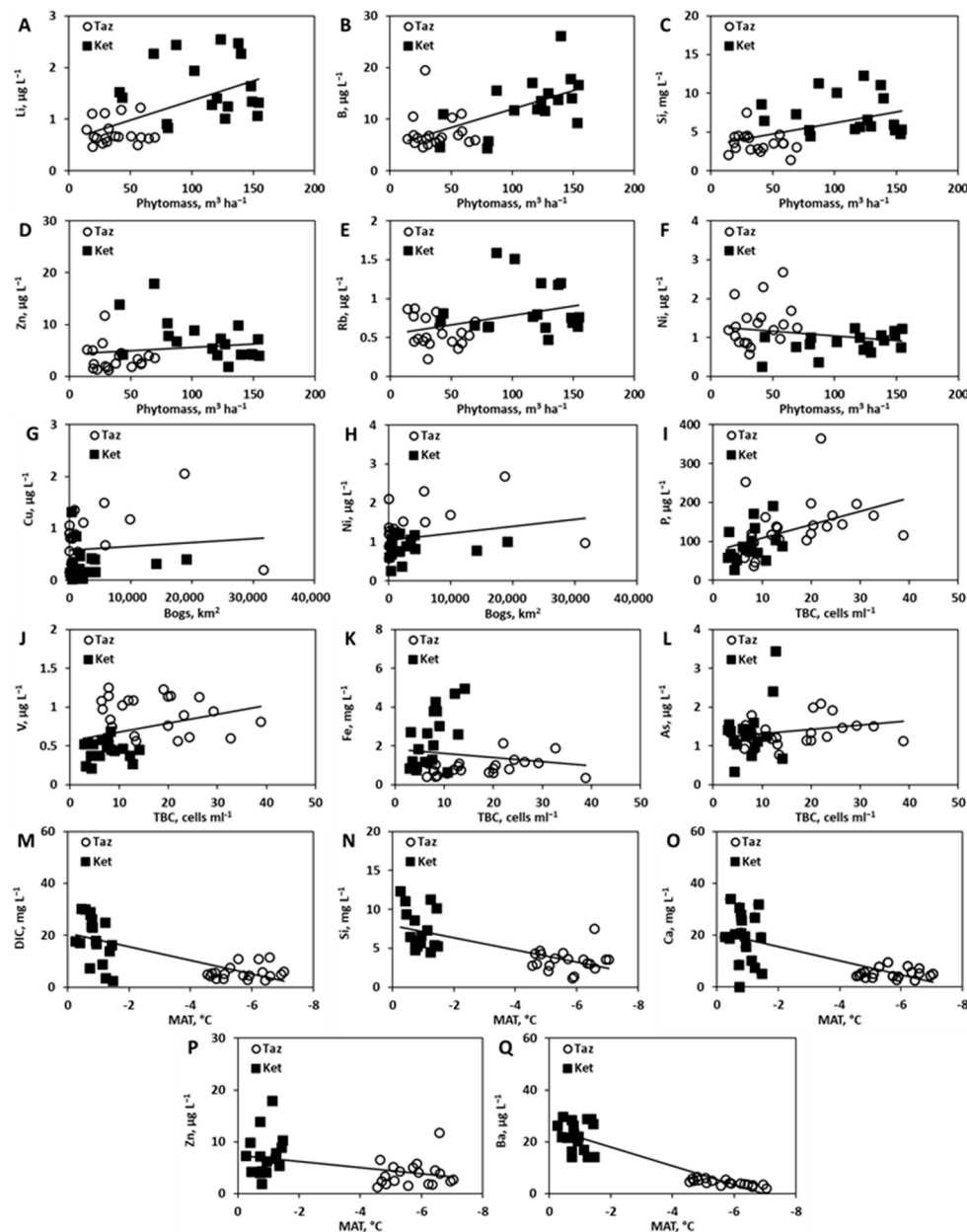


Figure 7. Pairwise correlations of several major and trace elements with two most pronounced landscape parameters—Phytomass stock at the watershed and bog coverage, total bacterial count (TBC) and mean air temperature, for both Taz and Ket river main stem and tributaries.

Given that the season was an important driving factor of element concentrations in the Ket River (see Section 3.1), we attempted a PCA treatment of elementary dataset of both rivers during summer baseflow. This analysis revealed three main factors capable of explaining 26, 14, and 6.6% of total variability, respectively (Figure S2, Table S6). The first factor acted positively on aluminum and other low mobile hydrolysates such as Be, Al, Ti, Cr, Ga, Y, Zr, Nb, Y, REE, Hf, Th and elements which are known to be strongly complexed with DOM such as Cu and Se [54]. Presumably, it reflected mobilization of low soluble elements from lithogenic (silicate) minerals in the form of organo-mineral (essentially organo-aluminum) colloids as it is known from studies in soil porewaters of the WSL regions [24]. The second factor negatively acted on labile Na, Mg, Si, Ca, P,

and Fe (probably as Fe(II)). The F2 was also positively linked to DOC, micronutrients (Zn, Rb, Ba), and phytomass at the watershed (primarily, light needle-leaf trees) as well as mean temperature and the proportion of younger (<25 Ma) rocks. In the WSL, these rocks contain carbonate concretions and partially carbonated loesses. The second factor thus likely represented a combined effect of productive litter in larch forest growing on carbonate-rich rocks and groundwater feeding of the rivers by soluble, highly mobile elements. Finally, the third factor, although exhibited limited explanation capacity, was strongly linked to pH, specific conductivity, DIC, Sr, and U and clearly marked a direct impact of bicarbonate-rich, slightly mineralized waters that reside in shallow (Taz) and deeper (Ket) subsurface reservoirs containing carbonate minerals and actively discharge into the river during baseflow.

Noteworthy is the similarity of the two main groups of major and trace elements, DOC- and DIC-related, based on pairwise correlations between element concentrations. The DIC concentration in both river basins significantly ($p < 0.05$) correlated with S.C., Si, alkalis (Li, Na), alkaline-earth metals (Mg, Ca, Sr, Ba), and U. This correlation marks an enhanced mobility of these elements in the form of ionic forms and neutral molecules (uranyl as carbonate/hydroxide complexes), essentially controlled by discharge of DIC and mobile element—rich groundwaters either at the river bank or in the hyporheic zone. These mechanisms of labile element mobilization are fairly well-known across the boreal zone [55]. The DOC correlated with trivalent (Sc, Al, Ga, Y, REE), tetravalent (Ti, Zr, Hf, Th), and other (Be, Cr, Nb) hydrolysates, Se and Cs. These elements are essentially present in the river water in the form of Al-organic colloids or organic complexes [14,54,56–58]. These two main groups of solutes were evidenced not only in large and small rivers and streams [14,16,17,20,59] but in lentic waters of the region, such as lakes and ponds [60,61], supra-permafrost waters [23], peat porewaters [22–24], and peat ice [21].

3.4. Climate Change Consequences on Element Concentration in WSL Rivers (Vegetation and Permafrost/Lithology Control) Using a Substituting Space for Time Approach

The main limitation of our approach is a restricted seasonal coverage in river sampling and lack of daily/weekly discharge measurements, which did not allow calculating elementary export fluxes (yields). As such, predictions of climate change impact on riverine export of this particular pristine basins can be performed solely in terms of river water hydrochemistry. Note however that an approach of element annual yields is well developed for other European Arctic [55] and small western Siberian rivers [13,59] including anthropogenically affected Ob River in its middle course [19]. Therefore, taking the advantage of highly pristine character of Taz and Ket River basins (in contrast to the neighboring Pur River basin and left tributaries of the Ob River, which are strongly impacted by gas and oil industry), one can use these river systems to approximate future changes in river hydrochemistry linked to on-going climate change and permafrost thaw. The validity of this approach is based on rather weak spatial variations within each basin discovered in the present study (notably over the course of the main stem but also among tributaries) in contrast to sizable variations in solute concentrations between the northern and southern river basin.

For this, we can employ a “substituting space for time” approach which postulates, in a broader context, that spatial phenomena which are observed today can be used to describe past and future events [62]. Such an approach has been successfully used in western Siberia since the pioneering work of Frey and Smith [12] to model possible future changes in small rivers [13,59], lakes [61], soil waters [23], and permafrost ice [21]. Indeed, with permafrost and forest boundary shift northward over next decades [9,63–65], the northern part of the Taz River (tundra and forest-tundra of continuous to discontinuous permafrost) can be entirely transformed into southern part-like territory of taiga and forest-tundra biome with discontinuous to sporadic permafrost, whereas the entire Ket River basin can be used as a surrogate for hydrochemistry for the southern part of the Taz River. The mean element concentrations in the main stem and tributaries in the two sub-basins of the Taz and Ket

River are illustrated in Figure 8. It can be seen that only a few elements exhibited sizable contrast in river water concentration between the southern and northern part of the Taz River basin and the Ket river catchment. Therefore, applying a substituting space for time approach, we can anticipate that the concentration of DIC and mobile elements (Li, B, Mg, Ca, Sr, Rb, Sb, W, U) and, to a lesser degree, DOC, Si, and micronutrients (Mn, Fe, Zn, Mo) will increase in the low reaches of the Taz River.

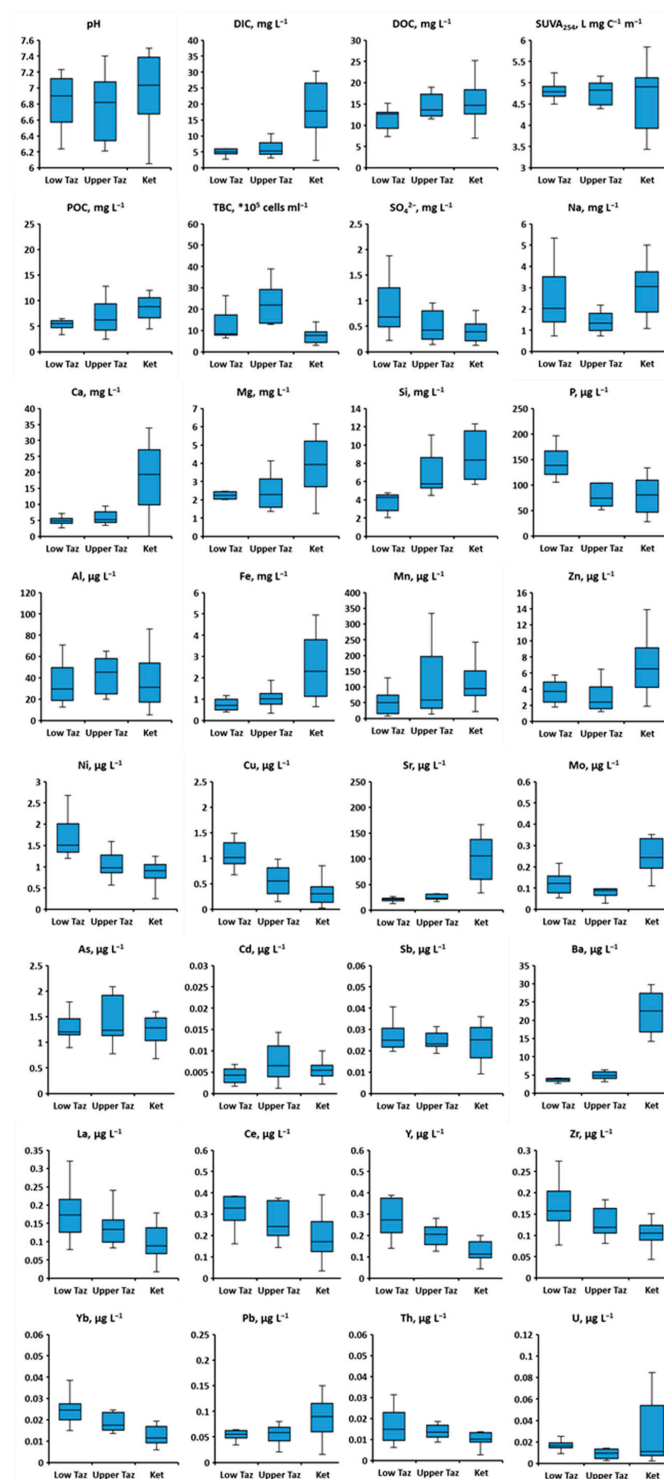


Figure 8. Elements concentration in Upper Taz (0–400 km from the mouth, northern part), Low Taz (400–800 km from the mouth, southern part), and Ket River (main stem and tributaries). Box represents median, whiskers correspond to lower and upper quartile.

Overall, the main consequences of the climate change in western Siberia on middle size river basin hydrochemistry seems to be primarily linked to the changes in dominant vegetation and biomass at the river watershed. In the northern part of the WSL, the change in hydrological pathways due to permafrost thaw might enrich the river waters in soluble elements due to enhanced underground water feeding (DIC, alkaline-earth elements (Ca, Sr), oxyanions (Mo, Sb), and U). The thickening of the active layer and enhanced involvement of thawed peat layer down to underlying mineral horizons may increase the export of trivalent and tetravalent hydrolysates in the form of organo-ferric colloids. However, at the short-term scale, due to two counterbalanced sources and sinks (permafrost thaw and plant uptake), the overall impact of the climate change on inorganic solute export by rivers from the land to the ocean may be smaller than that traditionally viewed for organic carbon.

4. Conclusions

Toward a better understanding of land cover control on dissolved (<0.45 μm) major and trace elements in the river water of high latitude regions, we selected two medium-size pristine rivers of the northern, permafrost-bearing and southern, permafrost-free region of the world's largest peatland, the Western Siberia Lowland (Taz and Ket River, respectively). We sampled the main stem and tributaries while encompassing a large gradient in river basin size, permafrost, and vegetation coverage at essentially similar lithological substrate, runoff, and relief. In the Ket River, the difference in major and trace solute concentration between two seasons was larger than the difference between the main stem and the tributaries. Given that the primary factor controlling the river solute concentration was the season, this allowed straightforward comparison of two river basins during the summer baseflow. Furthermore, sizable variations in solutes among different tributaries of each watershed (depending on land cover) allowed testing the impact of first-order environmental factors on river water hydrochemistry.

The similarity of landscape parameters (mainly, taiga vegetation, partially bogs and permafrost coverage, and, in a lesser degree, the lithology) controlled the major and trace element concentration pattern in two medium-size rivers studied in this work. A number of landscape parameters of the main stem and tributaries correlated with nutrients (B, Si, Zn, Rb, Ba with phytomass), low mobile lithogenic elements, and divalent transition metals whose transport is facilitated by high DOC (V, Ni, Cu, Y, heavy REE with bogs), or specific components reflecting bacterially controlled processing of DOM and groundwater discharge in the water column or within the hyporheic zone (Fe, P, SUVA, V, As). The mean annual air temperature encompassed the contrast between northern and southern rivers and correlated with labile elements of the river water (DIC, Li, B, Si, Ca, Sc, Zn, Se, Rb, Sb, Cs, Ba, and U), which was fully consistent with previous observations of large and small Siberian rivers.

Via quantitative comparison of element concentration along the south–north gradient of studied river basins and applying a substituting space for time approach, we infer that permafrost and vegetation shift northward may sizably (a factor of 2 to 3) enrich the river water in the north in highly mobile elements (DIC, Ca, Sr, U), and, in a lesser degree, in DOC, POC, and nutrients (Si, Mn, Zn, Fe, Mo), whereas the current concentrations of other macro (P) and micro-nutrients (V), and insoluble hydrolysates – geochemical tracers (Y, REE, Zr) in the low reaches of Taz might decrease.

Supplementary Materials: The following are available online at <https://www.mdpi.com/article/10.3390/w14142250/s1>, Figure S1: Seasonal mean \pm SD concentration elements exhibiting higher concentrations during spring flood compared to summer baseflow in tributaries and main channel Ket' in spring flood (blue) and summer (early fall) baseflow (orange). Figure S2: Results of PCA of ~65 hydrochemical and 16 land cover variables in ~ 60 sampling points of the main stem and tributaries of the Ket and Taz River basin, collected during summer baseflow. Table S1A. Mann-Whitney U Test comparison concentration in different season (flood vs. baseflow) in tributaries and main channel of the Ket River. Red color is for statistically significant differences. Table S1B. Mann-Whitney U

Test comparison concentration tributaries and main channel in different seasons. Table S2. Mean \pm SD concentrations of elements and other measured parameters in the Ket River main stem and tributaries. Table S3. Pairwise Pearson correlations of major and trace element concentrations in the Ket River (main stem and tributaries) during summer baseflow and main hydrochemical parameters of the water column and land cover. Significant ($p < 0.05$) correlations are given in red and most significant ($p < 0.01$) are highlighted in pink. Table S4. Hydrochemical parameters of the Taz River basin (stem and tributaries), July 2019. Table S5. Pearson pairwise correlations of major and trace elements of the river water (Taz and tributaries) with landscape parameters, vegetation coverage and climate. Significant ($p < 0.05$) correlations are given in red and most significant ($p < 0.01$) are highlighted in pink. Table S6. Results of PCA of ~65 hydrochemical and 16 land cover variables in ~60 sampling points of the main stem and tributaries of the Ket and Taz River basin, collected during summer baseflow. Significant ($p < 0.05$) correlations are given in red and most significant ($p < 0.01$) are highlighted in pink.

Author Contributions: O.S.P. designed the study and wrote the paper; A.G.L. and I.V.K. performed sampling, analysis, and their interpretation; S.N.V. and O.S.P. were responsible for the choice of sampling objects and statistical treatment. L.S.S. was in charge of DOC and bacterial analyses and their interpretation; M.A.K. provided the GIS data for river watersheds from available databases. All authors have read and agreed to the published version of the manuscript.

Funding: RSF grant 22-17-00253, RFBR grant 20-05-00729, the TSU Development Program “Priority-2030”, and grant “Kolmogorov” of MES (Agreement No 075-15-2022-241).

Informed Consent Statement: Not applicable.

Acknowledgments: We acknowledge support from RSF grant 22-17-00253, RFBR grant 20-05-00729, the TSU Development Program “Priority-2030”, and grant “Kolmogorov” of MES (Agreement No 075-15-2022-241).

Conflicts of Interest: The authors declare no conflict of interest.

References

1. Frey, K.E.; McClelland, J.W. Impacts of permafrost degradation on arctic river biogeochemistry. *Hydrol. Process.* **2009**, *23*, 169–182. [[CrossRef](#)]
2. Vonk, J.E.; Tank, S.E.; Bowden, W.B.; Laurion, I.; Vincent, W.F.; Alekseychik, P.; Amyot, M.; Billet, M.F.; Canário, J.; Cory, R.M.; et al. Reviews and Syntheses: Effects of permafrost thaw on arctic aquatic ecosystems. *Biogeosciences* **2015**, *12*, 7129–7167. [[CrossRef](#)]
3. Vonk, J.E.; Tank, S.E.; Walvoord, M.A. Integrating hydrology and biogeochemistry across frozen landscapes. *Nat. Commun.* **2019**, *10*, 5377. [[CrossRef](#)] [[PubMed](#)]
4. White, D.; Hinzman, L.; Alessa, L.; Cassano, J.; Chambers, M.; Falkner, K.; Francis, J.; Gutowski, W.J., Jr.; Holland, M.; Holmes, R.M.; et al. The arctic freshwater system: Changes and impacts. *J. Geophys. Res.* **2007**, *112*, G04S54. [[CrossRef](#)]
5. Barbieri, M.; Barberio, M.D.; Banzato, F.; Billi, A.; Boschetti, T.; Franchini, S.; Gori, F.; Petitta, M. Climate change and its effect on groundwater quality. *Environ. Geochem. Health* **2021**, 1–12. [[CrossRef](#)]
6. Eskandari, E.; Mohammadzadeh, H.; Nassery, H.; Vadiati, M.; Zadeh, A.M.; Kisi, O. Delineation of isotopic and hydrochemical evolution of karstic aquifers with different cluster-based (HCA, KM, FCM and GKM) methods. *J. Hydrol.* **2022**, *609*, 127706. [[CrossRef](#)]
7. Frey, K.E.; Smith, L.C. How well do we know northern land cover? Comparison of four global vegetation and wetland products with a new ground-truth database for West Siberia. *Glob. Biogeochem. Cycles* **2007**, *21*, GB1016. [[CrossRef](#)]
8. Kremenetsky, K.V.; Velichko, A.A.; Borisova, O.K.; MacDonald, G.M.; Smith, L.C.; Frey, K.E.; Orlova, L.A. Peatlands of the West Siberian Lowlands: Current knowledge on zonation, carbon content, and Late Quaternary history. *Quat. Sci. Rev.* **2003**, *22*, 703–723. [[CrossRef](#)]
9. Romanovsky, V.E.; Drozdov, D.S.; Oberman, N.G.; Malkova, G.V.; Kholodov, A.L.; Marchenko, S.S.; Moskalenko, N.G.; Sergeev, D.O.; Ukraintseva, N.G.; Abramov, A.A.; et al. Thermal state of permafrost in Russia. *Permafrost. Periglac. Processes* **2010**, *21*, 136–155. [[CrossRef](#)]
10. Smith, L.C.; Macdonald, G.M.; Velichko, A.A.; Beilman, D.W.; Borisova, O.K.; Frey, K.E.; Kremenetsky, K.V.; Sheng, Y. Siberian peatlands as a net carbon sink and global methane source since the early Holocene. *Science* **2004**, *303*, 353–356. [[CrossRef](#)]
11. Frey, K.E.; Siegel, D.I.; Smith, L.C. Geochemistry of west Siberian streams and their potential response to permafrost degradation. *Water Resour. Res.* **2007**, *43*, W03406. [[CrossRef](#)]
12. Frey, K.E.; Smith, L.C. Amplified carbon release from vast West Siberian peatlands by 2100. *Geophys. Res. Lett.* **2005**, *32*. [[CrossRef](#)]

13. Krickov, I.; Lim, A.; Manasypov, R.M.; Loiko, S.V.; Shirokova, L.S.; Kirpotin, S.N.; Karlsson, J.; Pokrovsky, O.S. Riverine particulate C and N generated at the permafrost thaw front: Case study of western Siberian rivers across a 1700-km latitudinal transect. *Biogeosciences* **2018**, *15*, 6867–6884. [[CrossRef](#)]
14. Krickov, I.V.; Pokrovsky, O.S.; Manasypov, R.M.; Lim, A.G.; Shirokova, L.S.; Viers, J. Colloidal transport of carbon and metals by western Siberian rivers during different seasons across a permafrost gradient. *Geochim. Cosmochim. Acta* **2019**, *265*, 221–241. [[CrossRef](#)]
15. Krickov, I.V.; Lim, A.G.; Manasypov, R.M.; Loiko, S.V.; Vorobyev, S.N.; Shevchenko, V.P.; Dara, O.M.; Gordeev, V.V.; Pokrovsky, O.S. Major and trace elements in suspended matter of western Siberian rivers: First assessment across permafrost zones and landscape parameters of watersheds. *Geochim. Cosmochim. Acta* **2020**, *269*, 429–450. [[CrossRef](#)]
16. Pokrovsky, O.S.; Manasypov, R.M.; Shirokova, L.S.; Loiko, S.V.; Krickov, I.V.; Kopysov, S.; Zemtsov, V.A.; Kulizhsky, S.P.; Vorobyev, S.N.; Kirpotin, S.N. Permafrost coverage, watershed area and season control of dissolved carbon and major elements in western Siberia rivers. *Biogeosciences* **2015**, *12*, 6301–6320. [[CrossRef](#)]
17. Pokrovsky, O.S.; Manasypov, R.M.; Loiko, S.; Krickov, I.A.; Kopysov, S.G.; Kolesnichenko, L.G.; Vorobyev, S.N.; Kirpotin, S.N. Trace element transport in western Siberia rivers across a permafrost gradient. *Biogeosciences* **2016**, *13*, 1877–1900. [[CrossRef](#)]
18. Vorobyev, S.N.; Pokrovsky, O.S.; Serikova, S.; Manasypov, R.M.; Krickov, I.V.; Shirokova, L.S.; Lim, A.; Kolesnichenko, L.G.; Kirpotin, S.N.; Karlsson, J. Permafrost boundary shift in Western Siberia may not modify dissolved nutrient concentrations in rivers. *Water* **2017**, *9*, 985. [[CrossRef](#)]
19. Vorobyev, S.N.; Pokrovsky, O.S.; Kolesnichenko, L.G.; Manasypov, R.M.; Shirokova, L.S.; Karlsson, J.; Kirpotin, S.N. Biogeochemistry of dissolved carbon, major, and trace elements during spring flood periods on the Ob River. *Hydrol. Processes* **2019**, *33*, 1579–1594. [[CrossRef](#)]
20. Kolesnichenko, I.; Kolesnichenko, L.G.; Vorobyev, S.N.; Shirokova, L.S.; Semiletov, I.P.; Dudarev, O.V.; Vorobev, R.S.; Shavrina, U.; Kirpotin, S.N.; Pokrovsky, O.S. Landscape, soil, lithology, climate and permafrost control on dissolved carbon, major and trace elements in the Ob River, western Siberia. *Water* **2021**, *13*, 3189. [[CrossRef](#)]
21. Lim, A.G.; Loiko, S.V.; Kuzmina, D.; Krickov, I.V.; Shirokova, L.S.; Kulizhsky, S.P.; Vorobyev, S.N.; Pokrovsky, O.S. Dispersed ground ice of permafrost peatlands: A non-accounted for source of C, nutrients and metals. *Chemosphere* **2021**, *266*, 128953. [[CrossRef](#)] [[PubMed](#)]
22. Raudina, T.V.; Loiko, S.V.; Lim, A.G.; Krickov, I.V.; Shirokova, L.S.; Istigichev, G.I.; Kuzmina, D.M.; Kulizhsky, S.P.; Vorobyev, S.N.; Pokrovsky, O.S. Dissolved organic carbon and major and trace elements in peat porewater of sporadic, discontinuous, and continuous permafrost zones of western Siberia. *Biogeosciences* **2017**, *14*, 3561–3584. [[CrossRef](#)]
23. Raudina, T.V.; Loiko, S.V.; Lim, A.; Manasypov, R.M.; Shirokova, L.S.; Istigichev, G.I.; Kuzmina, D.M.; Kulizhsky, S.P.; Vorobyev, S.N.; Pokrovsky, O.S. Permafrost thaw and climate warming may decrease the CO₂, carbon, and metal concentration in peat soil waters of the Western Siberia Lowland. *Sci. Total Environ.* **2018**, *634*, 1004–1023. [[CrossRef](#)]
24. Raudina, T.V.; Loiko, S.; Kuzmina, D.M.; Shirokova, L.S.; Kulizhsky, S.P.; Golovatskaya, E.A.; Pokrovsky, O.S. Colloidal organic carbon and trace elements in peat porewaters across a permafrost gradient in Western Siberia. *Geoderma* **2021**, *390*, 114971. [[CrossRef](#)]
25. Karlsson, J.; Serikova, S.; Vorobyev, S.N.; Rocher-Ros, G.; Denfeld, B.; Pokrovsky, O.S. Carbon emission from Western Siberian inland waters. *Nat. Commun.* **2021**, *12*, 825. [[CrossRef](#)]
26. Serikova, S.; Pokrovsky, O.S.; Ala-Aho, P.; Kazantsev, V.; Kirpotin, S.N.; Kopysov, S.G.; Krickov, I.V.; Laudon, H.; Manasypov, R.M.; Shirokova, L.S.; et al. High riverine CO₂ emissions at the permafrost boundary of Western Siberia. *Nat. Geosci.* **2018**, *11*, 825–829. [[CrossRef](#)]
27. Serikova, S.; Pokrovsky, O.S.; Laudon, H.; Krickov, I.V.; Lim, A.G.; Manasypov, R.M.; Karlsson, J. High carbon emissions from thermokarst lakes of Western Siberia. *Nat. Commun.* **2019**, *10*, 1552. [[CrossRef](#)]
28. Pokrovsky, O.; Lim, A.; Korets, M.; Krickov, I.; Vorobyev, S. Dissolved (<0.45 μm) major and trace elements and landscape parameters of Ket and Taz Rivers, Western Siberia. *Mendeley Data* **2022**, *V1*. [[CrossRef](#)]
29. Marie, D.; Partensky, F.; Vaulot, D.; Brussaard, C. Enumeration of phytoplankton, bacteria, and viruses in marine samples. *Curr. Protoc. Cytom.* **1999**, *10*, 11.11.1–11.11.5. [[CrossRef](#)]
30. Pokrovsky, O.S.; Manasypov, R.M.; Loiko, S.V.; Shirokova, L.S. Organic and organo-mineral colloids in discontinuous permafrost zone. *Geochim. Cosmochim. Acta* **2016**, *188*, 1–20. [[CrossRef](#)]
31. Shirokova, L.S.; Pokrovsky, O.S.; Kirpotin, S.N.; Desmukh, C.; Pokrovsky, B.G.; Audry, S.; Viers, J. Biogeochemistry of organic carbon, CO₂, CH₄, and trace elements in thermokarst water bodies in discontinuous permafrost zones of Western Siberia. *Biogeochemistry* **2013**, *113*, 573–593. [[CrossRef](#)]
32. Heimbürger, A.; Tharaud, M.; Monna, F.; Losno, R.; Desboeufs, K.; Nguyen, E.B. SLRS-5 elemental concentrations deduced from SLRS-5/SLRS-4 ratios of thirty-three uncertified elements. *Geostand. Geoanal. Res.* **2013**, *37*, 77–85. [[CrossRef](#)]
33. Yeghicheyan, D.; Bossy, C.; Bouhnik Le Coz, M.; Douchet, C.; Granier, G.; Heimbürger, A.; Lacan, F.; Lanzanova, A.; Rousseau, T.C.C.; Seidel, J.-L.; et al. A Compilation of Silicon, Rare Earth Element and Twenty-One other Trace Element Concentrations in the Natural River Water Reference Material SLRS-5 (NRC-CNRC). *Geostand. Geoanal. Res.* **2013**, *37*, 449–467. [[CrossRef](#)]
34. Bartalev, S.A.; Egorov, V.A.; Ershov, D.V.; Isaev, A.S.; Lupyan, E.A.; Plotnikov, D.E.; Uvarov, I.A. Remote mapping of vegetation land cover of Russia based on data of MODIS spectroradiometer. *Mod. Probl. Earth Remote Sens. Space* **2011**, *8*, 285–302. Available online: http://d33.infospace.ru/d33_conf/2011v8n4/285-302.pdf (accessed on 15 June 2022).

35. Harris, I.; Jones, P.D.; Osborn, T.J.; Lister, D.H. Updated high-resolution grids of monthly climatic observations—The CRU TS3.10 Dataset. *Int. J. Climatol.* **2014**, *34*, 623–642. [[CrossRef](#)]
36. Hugelius, G.; Tarnocai, C.; Broll, G.; Canadell, J.G.; Kuhry, P.; Swanson, D.K. The Northern Circumpolar Soil Carbon Database: Spatially distributed datasets of soil coverage and soil carbon storage in the northern permafrost regions. *Earth Syst. Sci. Data* **2013**, *5*, 3–13. [[CrossRef](#)]
37. Santoro, M.; Beer, C.; Cartus, O.; Schullius, C.; Shvidenko, A.; McCallum, I.; Wegmueller, U.; Wiesmann, A. The BIOMASAR algorithm: An approach for retrieval of forest growing stock volume using stacks of multi-temporal SAR data. In Proceedings of the ESA Living Planet Symposium, Bergen, Norway, 28 June–2 July 2010. Available online: <https://www.researchgate.net/publication/230662433> (accessed on 15 June 2022).
38. Krickov, I.V.; Lim, A.G.; Shevchenko, V.P.; Vorobyev, S.N.; Candaudap, F.; Pokrovsky, O.S. Dissolved metal (Fe, Mn, Zn, Ni, Cu, Co, Cd, Pb) and metalloid (As, Sb) in snow water across a 2800-km latitudinal profile of western Siberia: Impact of local pollution and global transfer. *Water* **2022**, *14*, 94. [[CrossRef](#)]
39. Barker, A.J.; Douglas, T.A.; Jacobson, A.D.; McClelland, J.W.; Ilgen, A.G.; Khosh, M.S.; Lehn, G.O.; Trainor, T.P. Late season mobilization of trace metals in two small Alaskan arctic watersheds as a proxy for landscape scale permafrost active layer dynamics. *Chem. Geol.* **2014**, *381*, 180–193. [[CrossRef](#)]
40. Keller, K.; Blum, J.D.; Kling, G.W. Geochemistry of soils and streams on surfaces of varying ages in arctic Alaska. *Arct. Antarct. Alp. Res.* **2007**, *39*, 84–98. [[CrossRef](#)]
41. Keller, K.; Blum, J.D.; Kling, G.W. Stream geochemistry as an indicator of increasing permafrost thaw depth in an arctic watershed. *Chem. Geol.* **2010**, *273*, 76–81. [[CrossRef](#)]
42. Laudon, H.; Sjöblom, V.; Buffam, I.; Seibert, J.; Morth, M. The role of catchment scale and landscape characteristics for runoff generation of boreal streams. *J. Hydrol.* **2007**, *344*, 198–209. [[CrossRef](#)]
43. Viers, J.; Prokushkin, A.S.; Pokrovsky, O.S.; Beaulieu, E.; Oliva, P.; Dupré, B. Seasonal and spatial variability of elemental concentrations in boreal forest larch foliage of Central Siberia on continuous permafrost. *Biogeochemistry* **2013**, *113*, 435–449. [[CrossRef](#)]
44. Lidman, F.; Morth, C.M.; Laudon, H. Landscape control of uranium and thorium in boreal streams—Spatiotemporal variability and the role of wetlands. *Biogeosciences* **2012**, *9*, 4773–4785. [[CrossRef](#)]
45. Lidman, F.; Kohler, S.J.; Morth, C.-M.; Laudon, H. Metal transport in the boreal landscape—The role of wetlands and the affinity for organic matter. *Environ. Sci. Technol.* **2014**, *48*, 3783–3790. [[CrossRef](#)]
46. Ingri, J.; Widerlund, A.; Land, M.; Gustafsson, Ö.; Andersson, P.S.; Öhlander, B. Temporal variations in the fractionation of the rare earth elements in a boreal river, the role of colloidal particles. *Chem. Geol.* **2000**, *166*, 23–45. [[CrossRef](#)]
47. Stolpe, B.; Guo, L.; Shiller, A.M.; Aiken, G.R. Abundance, size distribution and trace-element binding of organic and iron-rich nanocolloids in Alaskan rivers, as revealed by field-flow fractionation and ICP-MS. *Geochim. Cosmochim. Acta* **2013**, *105*, 221–239. [[CrossRef](#)]
48. Vasyukova, E.V.; Pokrovsky, O.S.; Viers, J.; Oliva, P.; Dupré, B.; Martin, F.; Candaudap, F. Trace elements in organic- and iron-rich surficial fluids of the boreal zone: Assessing colloidal forms via dialysis and ultrafiltration. *Geochim. Cosmochim. Acta* **2010**, *74*, 449–468. [[CrossRef](#)]
49. Oleinikova, O.; Drozdova, O.Y.; Lapitskiy, S.A.; Demin, V.V.; Bychkov, A.Y.; Pokrovsky, O.S. Dissolved organic matter degradation by sunlight coagulates organo-mineral colloids and produces low-molecular weight fraction of metals in boreal humic waters. *Geochim. Cosmochim. Acta* **2017**, *211*, 97–114. [[CrossRef](#)]
50. Oleinikova, O.; Shirokova, L.S.; Gérard, E.; Drozdova, O.Y.; Lapitskiy, S.A.; Bychkov, A.Y.; Pokrovsky, O.S. Transformation of organo-ferric peat colloids by a heterotrophic bacterium. *Geochim. Cosmochim. Acta* **2017**, *205*, 313–330. [[CrossRef](#)]
51. Shirokova, L.S.; Bredoire, R.; Rolls, J.-L.; Pokrovsky, O.S. Moss and peat leachate degradability by heterotrophic bacteria: Fate of organic carbon and trace metals. *Geomicrobiol. J.* **2017**, *34*, 641–655. [[CrossRef](#)]
52. Shirokova, L.S.; Chupakova, A.A.; Chupakov, A.V.; Pokrovsky, O.S. Transformation of dissolved organic matter and related trace element in the mouth zone of the largest European Arctic river: Experimental modeling. *Inland Waters* **2017**, *7*, 272–282. [[CrossRef](#)]
53. Vorobyev, S.N.; Kolesnichenko, Y.; Korets, M.; Pokrovsky, O.S. Testing landscape, climate and lithology impact on carbon, major and trace elements of the Lena River and its tributaries during a spring flood period. *Water* **2021**, *13*, 2093. [[CrossRef](#)]
54. Pokrovsky, O.S.; Bueno, M.; Manasyrov, R.M.; Shirokova, L.S.; Karlsson, J.; Amouroux, D. Dissolved organic matter controls on seasonal and spatial selenium concentration variability in thaw lakes across a permafrost gradient. *Environ. Sci. Technol.* **2018**, *52*, 10254–10262. [[CrossRef](#)] [[PubMed](#)]
55. Chupakov, A.V.; Pokrovsky, O.S.; Moreva, O.Y.; Shirokova, L.S.; Neverova, N.V.; Chupakova, A.A.; Kotova, E.I.; Vorobyeva, T.Y. High resolution multi-annual riverine fluxes of organic carbon, nutrient and trace element from the largest European Arctic river, Severnaya Dvina. *Chem. Geol.* **2020**, *538*, 119491. [[CrossRef](#)]
56. Bagard, M.L.; Chabaux, F.; Pokrovsky, O.S.; Prokushkin, A.S.; Viers, J.; Dupré, B.; Stille, P.; Rihs, S.; Schmitt, A.-D. Seasonal variability of element fluxes in two Central Siberian rivers draining high latitude permafrost dominated areas. *Geochim. Cosmochim. Acta* **2011**, *75*, 3335–3357. [[CrossRef](#)]
57. Dahlqvist, R.; Andersson, K.; Ingri, J.; Larsson, T.; Stolpe, B.; Turner, D. Temporal variations of colloidal carrier phases and associated trace elements in a boreal river. *Geochim. Cosmochim. Acta* **2007**, *71*, 5339–5354. [[CrossRef](#)]

58. Lyvén, B.; Hassellöv, M.; Turner, D.R.; Haraldsson, C.; Andersson, K. Competition between iron- and carbon-based colloidal carriers for trace metals in a freshwater assessed using flow field-flow fractionation coupled to ICPMS. *Geochim. Cosmochim. Acta* **2003**, *67*, 3791–3802. [[CrossRef](#)]
59. Pokrovsky, O.S.; Manasypov, R.M.; Kopysov, S.; Krickov, I.V.; Shirokova, L.S.; Loiko, S.V.; Lim, A.G.; Kolesnichenko, L.G.; Vorobyev, S.N.; Kirpotin, S.N. Impact of permafrost thaw and climate warming on riverine export fluxes of carbon, nutrients and metals in western Siberia. *Water* **2020**, *12*, 1817. [[CrossRef](#)]
60. Manasypov, R.M.; Vorobyev, S.N.; Loiko, S.V.; Kritzkov, I.V.; Shirokova, L.S.; Shevchenko, V.P.; Kirpotin, S.N.; Kulizhsky, S.P.; Kolesnichenko, L.G.; Zemtsov, V.A.; et al. Seasonal dynamics of organic carbon and metals in thermokarst lakes from the discontinuous permafrost zone of western Siberia. *Biogeosciences* **2015**, *12*, 3009–3028. [[CrossRef](#)]
61. Manasypov, R.M.; Lim, A.G.; Krickov, I.V.; Shirokova, L.S.; Vorobyev, S.N.; Kirpotin, S.N.; Pokrovsky, O.S. Spatial and seasonal variations of C, nutrient, and metal concentration in thermokarst lakes of Western Siberia across a permafrost gradient. *Water* **2020**, *12*, 1830. [[CrossRef](#)]
62. Blois, J.L.; Williams, J.W.; Fitzpatrick, M.C.; Jackson, S.T.; Ferrier, S. Space can substitute for time in predicting climate-change effects on biodiversity. *Proc. Natl. Acad. Sci. USA* **2013**, *110*, 9374–9379. [[CrossRef](#)] [[PubMed](#)]
63. García Criado, M.; Myers-Smith, I.H.; Bjorkman, A.D.; Lehmann, C.E.R.; Stevens, N. Woody plant encroachment intensifies under climate change across tundra and savanna biomes. *Glob. Ecol. Biogeogr.* **2020**, *29*, 925–943. [[CrossRef](#)]
64. Mauclet, E.; Agnan, Y.; Hirst, C.; Monhonval, A.; Pereira, B.; Vandeuren, A.; Villani, M.; Ledman, J.; Taylor, M.; Jasinski, B.L.; et al. Changing sub-Arctic tundra vegetation upon permafrost degradation: Impact on foliar mineral element cycling. *Biogeosciences* **2022**, *19*, 2333–2351. [[CrossRef](#)]
65. Tape, K.; Sturm, M.; Racine, C. The evidence for shrub expansion in Northern Alaska and the Pan-Arctic. *Glob. Change Biol.* **2006**, *12*, 686–702. [[CrossRef](#)]